Clim Dyn (2006) 27:815–830
DOI 10.1007/s00382-006-0164-2

Intraseasonal variations of the Yangtze rainfall and its related atmospheric circulation features during the 1991 summer

Jiangyu Mao · Guoxiong Wu

Received: 19 September 2005 / Accepted: 25 May 2006 / Published online: 23 June 2006

Abstract The intraseasonal variations of the Yangtze rainfall over eastern China and its related atmospheric circulation characteristics during the 1991 summer are examined based on the gauge-observed rainfall and the NCEP/NCAR reanalysis data. Wavelet analysis shows that during the 1991 summer, the active and break sequences of rainfall over the middle and lower Yangtze Basin are mainly regulated by an oscillatory mode with a period of 15–35 days. An investigation of the circulation features suggests that the 15–35-day oscillation is associated with an anomalous low-level cyclone (anticyclone) appearing alternatively over the northern South China Sea (SCS) and the Philippine Sea, and related to a northeastward (southwestward) shift of the western Pacific subtropical anticyclone over the SCS, leading to a lower tropospheric divergence (convergence) over the Yangtze Basin. In the upper troposphere, the 15–35-day oscillation exhibits a dipole anomaly characterized by an anomalous cyclone (anticyclone) over eastern China and an anomalous anticyclone (cyclone) over the northern Tibetan Plateau, resulting in a southwestward shrinking (northeastward extending) of the South Asian anticyclone, and forming a convergence (divergence) over eastern China. Such a coupled anomalous flow pattern between the lower and upper troposphere favors large-scale descending (ascending) motion, and hence reduced (enhanced) rainfall over the Yangtze Basin. Dynamically, the intraseasonal variations in the Yangtze rainfall are mainly determined by the coupling between the low-level relative vorticity and the upper-level divergence. In the middle troposphere, the 15–35-day oscillation of the subtropical high is originated over the central North Pacific north of Hawaii, then propagates westward to the SCS-Philippine Sea, and finally modulates the intraseasonal variations of the Yangtze rainfall.

J. Mao (✉) · G. Wu
State Key Laboratory of Numerical Modeling for Atmospheric Sciences and Geophysical Fluid Dynamics (LASG), Institute of Atmospheric Physics, Chinese Academy of Sciences, P.O. Box 9804, Beijing 100029, China
e-mail: mjy@lasg.iap.ac.cn

1 Introduction

Broadly speaking, the East Asian monsoon covers a much large area spanning from the equatorial regions of the Southeast Asia and the South China Sea (SCS) to northeastern China, Japan, and Korea (Lau et al. 1988; Lau and Yang 1996). In a narrow sense, the East Asian monsoon only refers to the subtropical monsoon that covers extratropical East Asia, prevailing over the Yangtze Basin through northeastern China into Korea and Japan. Thus, Chen et al. (2000) suggested that the East Asian summer monsoon is mainly characterized by the Meiyu (in eastern China)-Baiu (in Japan) front, which is climatologically one of the major convergence zones within the global atmospheric circulation. Tao and Chen (1987) presented a schematic diagram of the components of the East Asian summer monsoon system (see their Fig. 8), in which the climatological positions of the monsoon trough and Meiyu front are shown clearly. The distributions of summer rainfall over eastern China exhibit three east–west oriented heavy rainbands that are related to the northward shift

of the Meiyu front across the Yangtze River (Tao and Ding 1981). In climatology, the Meiyu front is generally established around mid-June, triggering the onset of heavy summer monsoon rain over the Yangtze Basin, and then migrates northward. However, this intraseasonal spatial-temporal evolution undergoes large interannual variations so that a flood condition may result from a heavier-than-normal rainfall during the normal rain period or from sustained rain outside of the normal period or both (Chang et al. 2000a). It is well known that the period 1991–1993 featured a prolonged El Niño episode. Although the central equatorial Pacific sea surface temperature (SST) anomalies kept positive throughout much of 1990 and early 1991, this El Niño event really began around the beginning of May, with warm SST anomalies exceeding 0.5°C in the central and eastern Pacific, and reached its peak phase in the first quarter of 1992 (McPhaden 1993). Under anomalous climate background of the El Niño event, the onset of the 1991 Yangtze Meiyu was one month earlier than normal, the rain period lasted much longer than normal, and excessive summer total rainfall led to severe floods. These suggest that the El Niño event has significant influences on weather and climate anomalies over China through interrupting the normal seasonal evolution of the oceanic/atmospheric system. Note that the 1991 summer coincided with the developing phase of the El Niño event. Based on data from 1950 to 1980, Huang and Wu (1989) suggested that the developing stage of a warm El Niño-South Oscillation (ENSO) event is generally associated with an excessive summer rainfall over the Yangtze Basin and a deficient one over southern and northern China.

In addition to association with the El Niño event, the 1991 East Asian summer monsoon exhibited anomalous characteristics in terms of distinct intraseasonal variability. In 1991, the Yangtze Meiyu started around 18 May, and lasted until mid-July (Lu and Ding 1997). Within such a longer Meiyu period the Yangtze rainfall intensity exhibited several break and active periods, indicating strong intraseasonal oscillations (ISOs). A series of heavy rain events occurred over the middle and lower Yangtze Basin, and resulted in devastating floods and severe economic losses. As suggested by Webster et al. (1998), agricultural practices have traditionally been tied strictly to the annual cycle. Small variations in the timing and quantity of rainfall have the potential for significant societal consequences. Therefore, in addition to the importance of the strength of the overall summer monsoon in a particular year, forecasting the subseasonal variability of the monsoon is an issue of considerable urgency. Due to unusual features in terms of the El Niño background, extreme floods, and significant ISOs, the 1991 summer is selected to illustrate the atmospheric circulation characteristics relevant to the evolution and maintenance of the extratropical East Asian summer monsoon.

It is thought that the Meiyu front results from the convergence between tropical flow from the warm oceans and cold air from the middle–high latitudes, and tropical–extratropical interaction is an inherent property of the East Asian monsoon (e.g., Tanaka 1992; Fukutomi and Yasunari 1999, 2002; Hsu 2005). Lau et al. (1988) surveyed the seasonal and intraseasonal progression relevant to the establishment and shift of the Meiyu front over eastern China, and suggested that the northward progression and the rapid transitions of the major rainbands may result from the phase lock between the 40- and 20-day ISO modes. Chen et al. (2000) showed an opposite-phase intraseasonal variation existing between the SCS and Yangtze Basin based on the temporal evolutions of the filtered monsoon indices represented by outgoing longwave radiation and 850-hPa zonal winds. Zhu et al. (2003) reported that the 1998 floods over eastern China was related to the activity of the 30–60-day ISOs over the western North Pacific, where the monsoon trough and the subtropical anticyclone appeared as an anticlockwise propagation with enhanced and suppressed convective anomalies in a 30–60-day period. Mao and Chan (2005) proposed that the 30–60-day and 10–20-day ISO modes control the behavior of the SCS summer monsoon for most of years. The 30–60-day mode exhibits a trough-ridge seesaw over the SCS, with anomalous cyclones (anticyclones) along with enhanced (suppressed) convection migrating northward. Such a seesaw phenomenon manifests among three latitudinal locations involving the equator, central SCS, and Yangtze Basin during the peak phases, suggesting the linkage between the tropics and extratropics on intraseasonal timescale.

Previous studies have emphasized the impacts of the western Pacific subtropical high (WPSH) on the monsoon (e.g., Tao and Zhu 1964; Chang et al. 2000a, b) because it separates the Meiyu front from the SCS monsoon trough that stretches from northern Indochina Peninsula to the Philippine Sea. Tao and Chen (1987) pointed out that both the WPSH in the middle and lower troposphere and the South Asian high in the upper troposphere are important components of the East Asian monsoon system. The meridional and/or zonal shift of the WPSH ridge influences the location where the southeasterlies to its south converge with the southwesterlies associated with the Somali cross-equatorial flow, and hence the summer monsoon rainfall. On the other hand, an interactive relationship

between the summer monsoon and the subtropical high on longer than monthly time scales have also been documented (e.g., Hoskins 1996; Wu et al. 1999; Wu and Liu 2003). Rodwell and Hoskins (2001) pointed out that deep convective condensation heating related to the summer monsoon might contribute to the formation and variation of the subtropical anticyclone. Liu et al. (2001) found that the latent heating released by the Asian summer monsoon rainfall is a key factor in forming summer subtropical anticyclone in the Eastern Hemisphere. Yeh et al. (1959) suggested that during the Meiyu onset, the large-scale summer circulation over East Asia undergoes some abrupt changes, in which the rapid northward shift of the upper-level westerlies across the Tibetan Plateau is one of the most significant features, implying that the Yangtze summer rainfall may be linked with the variations in the middle and upper tropospheric circulations on intraseasonal time scales. Therefore, the objective of this paper is to examine the intraseasonal variations of the Yangtze rainfall during the 1991 summer through a detail analysis on the temporal-spatial structures of the atmospheric circulation associated with these intraseasonal events, which may lead to a better understanding on the causes of the 1991 extreme floods over the Yangtze Basin.

The data and method used in this study are described in Sect. 2. Evolution of large-scale atmospheric circulation and rainfall in the summer of 1991 are presented in Sect. 3. The active and break periods which characterized the 1991 rainy season are identified in Sect. 4, and the intraseasonal relationships between the Yangtze rainfall and circulation fields are also investigated. The summary and discussion follow in Sect. 5.

2 Data and methodology

2.1 Data

The primary datasets used in this study are the daily mean data from the National Centers for Environmental Prediction/National Center for Atmospheric Research (NCEP/NCAR) reanalysis (Kalnay et al. 1996), which include wind, geopotential height, temperature, vertical velocity, and relative humidity at 17 standard pressure levels, with a horizontal resolution of 2.5° latitude × 2.5° longitude grid. The daily long-term mean are calculated for the period 1968–1996, which are obtained directly from the website of the NOAA-CIRES Climate Diagnostics Center.

Daily rain-gauge precipitation data over China during 1951–1998 are provided by the Climate Data Center, China Meteorological Administration. They are used to examine the climatological seasonal march of rainbelt over eastern China and the 1991 summer precipitation characteristics. The rainfall index is defined by area-averaged rainfall over the middle and lower Yangtze Basin, and used to identify the ISOs of the Yangtze rainfall during the 1991 summer. The summer season here is defined as the period from 1 May to 31 August. The intraseasonal variability of the Yangtze rainfall is analyzed by applying wavelet analysis for determining the dominant intraseasonal periods.

2.2 Wavelet analysis and filtering

Wavelet analysis, which is a common tool for diagnosing time–frequency variations of a time series, is performed to identify the dominant ISO modes. Since the wavelet transform is a bandpass filter with a known response function (the wavelet function), it is also a powerful filtering technique (e.g. Lau and Weng 1995; Torrence and Compo 1998; Chan et al. 2002; Mao and Chan 2005). The time series of the ISO component can be reconstructed by the inverse transform over a range of scales. The wavelet analysis method is therefore employed to isolate the ISO components. Because the time series of the Yangtze rainfall exhibits significant oscillatory behavior with sharp jump, based on the choice principle of the wavelet function, the wavelet basis function selected here is the m-order derivatives of a Gaussian (Torrence and Compo 1998), where m is chosen to be six. Such a real wavelet function returns only a single component and is suitable to isolate peaks or discontinuities. The gridded fields of other daily meteorological quantities such as 850-hPa winds are also filtered with the wavelet transform to extract the ISO components.

3 Characteristics of rainfall and large-scale atmospheric circulation during summer

3.1 Precipitation

The precipitation amount during summer season is one of the most important indicators of the East Asian summer monsoon. Figure 1 shows the distributions of the summer rainfall in climate mean and in 1991. The maximum rainfall (exceeding 800 mm) regions are mostly confined to the southern and southeastern China near the coast (Fig. 1a). Along the Yangtze

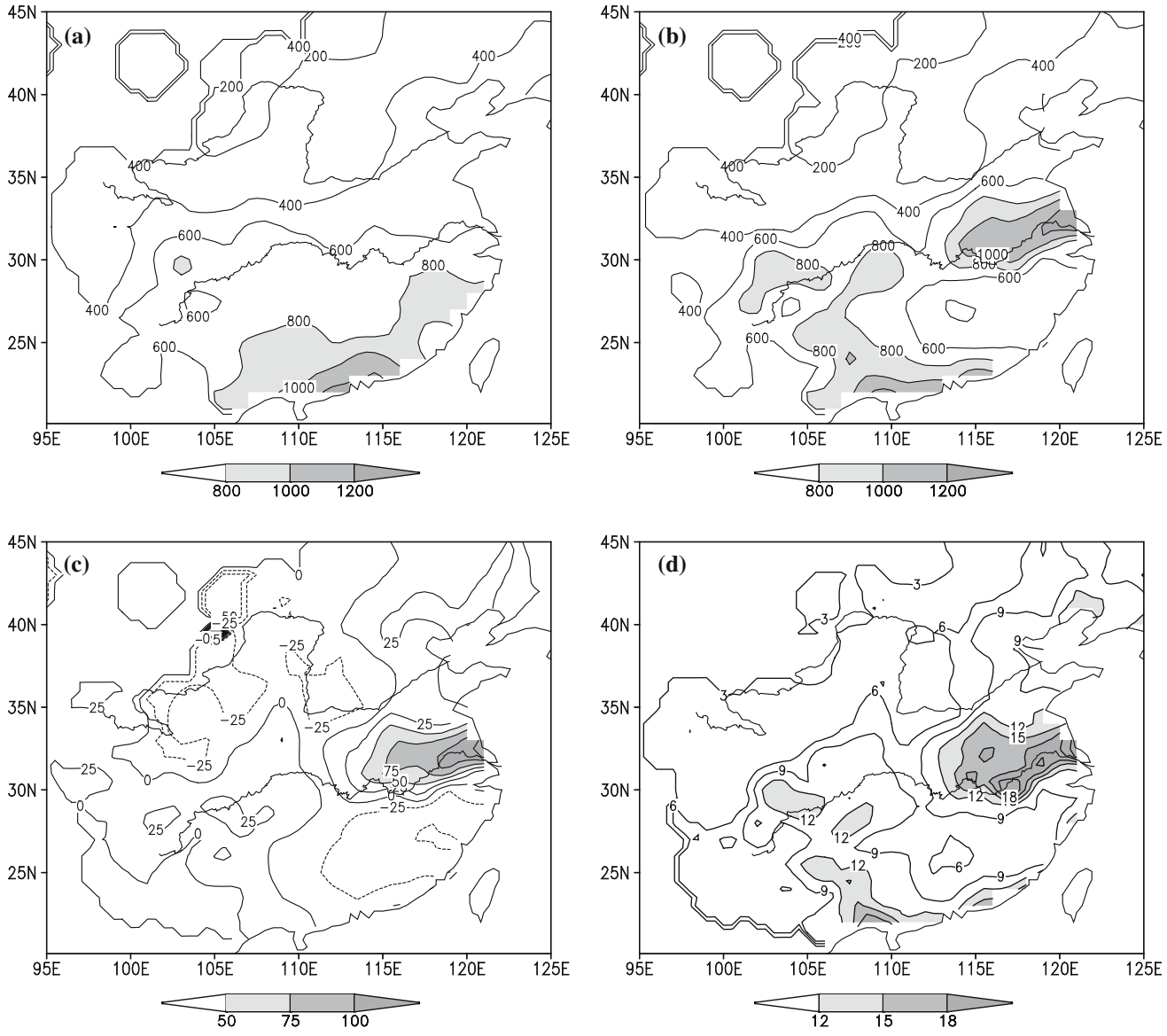

Fig. 1 Distributions of the summer (1 May–31 August) rainfall (mm) for **a** climatology and **b** 1991; **c** the 1991 summer percentage departure from the climatological rainfall (%); **d** the subseasonal standard deviation (mm day^{-1}) for the 1991 summer. The climatology is based on the period 1951–1998

River the rainfall amount is around 600 mm, while over northern China it drops to below 400 mm. The entire climatological rainfall pattern basically exhibits a degression tendency from southeastern to northwestern China. Note that singular isoline distributions occur over northwestern China, which results from the data interpolation based on sparse observational stations over there. Similar situation thus exists during the 1991 summer. However, this will not affect our present discussion since we only focus on the region of eastern China where enough dense station observations are available. During the summer of 1991 (Fig. 1b), the total summer rainfall at many stations along the Yangtze valley exceeds 600 mm, while over its middle and lower Basin the amount even exceeds 1,000 mm, resulting in severe floods there. Based on the percentage departure from the climatological mean, the rainfall anomalies could be clearly revealed. Positive rainfall anomalies exceeding 50% are found over the middle and lower Yangtze Basin (Fig. 1c). To a certain extent, subseasonal standard deviations could reflect the strength of the intraseasonal rainfall variability. The standard deviation for each individual station is calculated based on the daily rainfall anomaly, and this

anomaly is defined as departure from the average for the period 1 May to 31 August 1991. The rainfall anomaly maximum over the middle and lower Yangtze Basin is concurrent with maximum of the subseasonal standard deviation in excess of 15 mm day^{-1} (Fig. 1d), which indicates that the temporal evolutions of the 1991 Yangtze rainfall is largely modulated by strong ISOs.

3.2 Wind and geopotential height

Since the rainfall over the Yangtze Basin is mostly produced from the Meiyu front, the three-dimensional structure of the atmospheric circulation should be portrayed. Figure 2 displays the summer mean and anomalous wind fields for the lower, middle, and upper troposphere. Previous studies (e.g., Huang and Yue

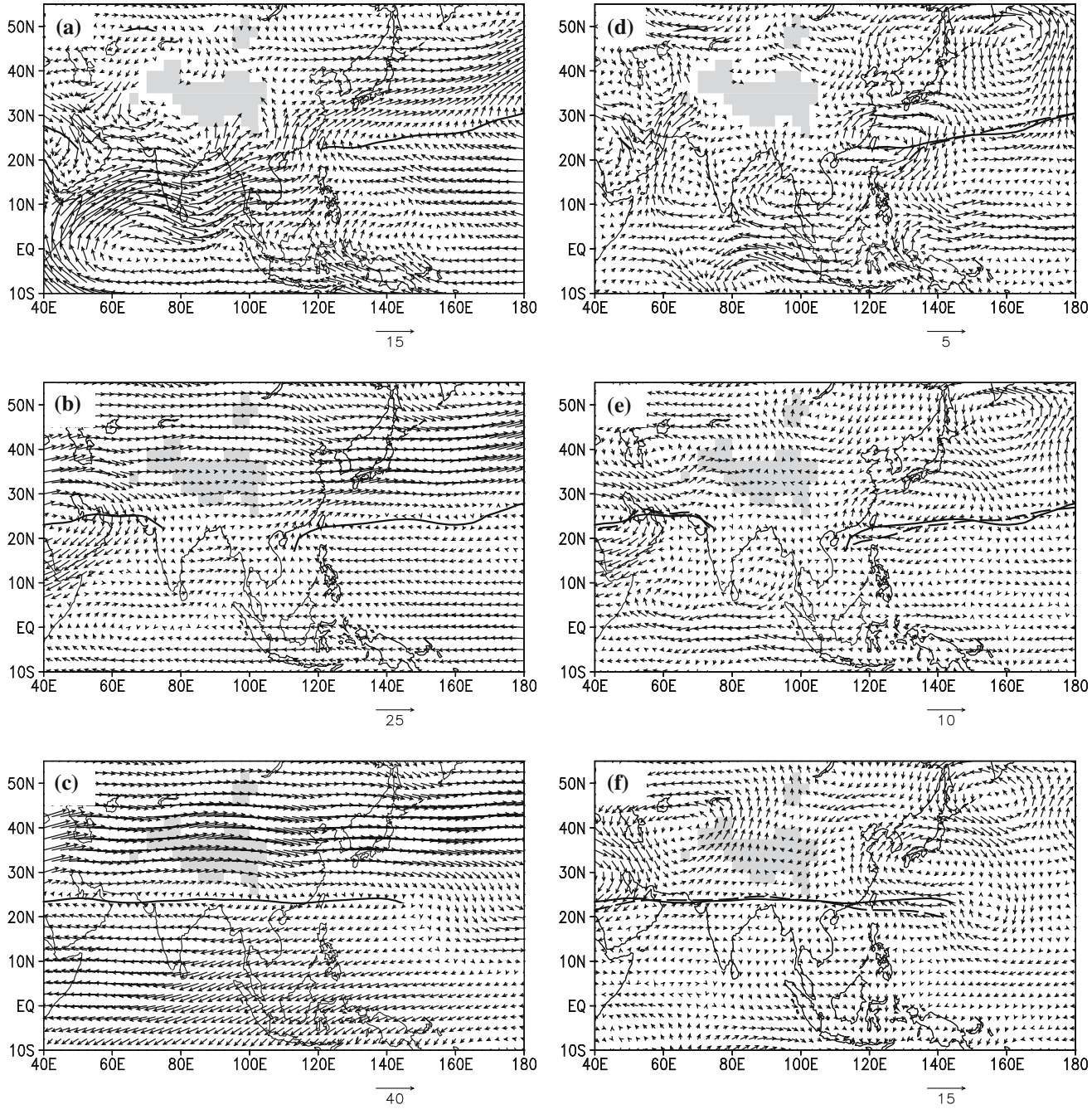

Fig. 2 Mean (*left panel*) and anomalous (*right panel*) large-scale circulations (m s^{-1}) for the 1991 summer. **a**, **d** 850-hPa winds, **b**, **e** 500-hPa winds, **c**, **f** 200-hPa winds. Anomalies are calculated as departures from the 1968 to 1996 base period seasonal means. *Thick solid* (*dashed*) *line* denotes the subtropical anticyclone ridgeline for the summer of 1991 (climatology). *Shading* indicates the Tibetan Plateau above 1,500 m

1962; Tao and Chen 1987) showed that the establishment of the Meiyu front is sensitive to the location of the western North Pacific subtropical anticyclone. During the Meiyu period, the 500-hpa subtropical anticyclone relatively stabilizes with its ridgeline locating between 20 and 25°N. Thus the ridgeline is plotted on the wind or geopotential height field to highlight the main body of the subtropical anticyclone. The low-level winds show a considerable convergence zone over the Yangtze Basin, which could be identified by abrupt degression of strong southerlies along 30°N (Fig. 2a). The typical monsoon southwesterlies from the Somali cross-equatorial flow across the Indochina Peninsula converge with the southeasterlies on the southern flank of the western Pacific anticyclone in such a way that the warm moist airflow is advected toward the Meiyu front, leading to heavy rain over the Yangtze Basin. Note that the subtropical anticyclone ridgeline situates around 25°N, with its westernmost point being located around 120°E. Similar to the 850-hPa flow pattern, the subtropical anticyclone in the 500-hPa wind field is dominant over the western North Pacific (Fig. 2b). The 500-hPa WPSH is generally considered as a key system for the East Asian weather and climate (e.g., Tao and Zhu 1964; Chang et al. 2000a, b), because it is an important indicator in forecasting the onset and termination of the Meiyu. It is found that the ridgeline just situates between 20 and 25°N, implying that the subtropical anticyclone frequently stagnated within this latitude band during summer. In the upper troposphere, a huge anticyclone is centered over the southern Tibetan Plateau, with its ridgeline locating along 24°N (Fig. 2c). The vertical meridional circulation within the longitudes of eastern China is identified by the upper tropospheric northerlies over the eastern part of the South Asian anticyclone and the lower tropospheric southerlies (Fig. 2a). This vertical circulation favors an occurrence of rainfall over the Yangtze Basin. Moreover, the persistent maintenance of the western Pacific subtropical anticyclone in the middle troposphere is also conducive to enhanced rainfall over the Yangtze Basin.

An investigation of the wind anomalies can help us to understand how the monsoon anomaly is in the summer of 1991. To reveal the location of the anomaly occurring within the WPSH, the summer WPSH ridgelines in climatology and in 1991 are superimposed on the wind anomaly field for comparison. In the lower troposphere, an anomalous anticyclone is present over the East China Sea, while the subtropical anticyclone ridgeline in 1991 almost overlaps with the climatological mean, indicating the intensification of the WPSH (Fig. 2d). Notice that there are significant westerly anomalies over the equatorial western Pacific, which reflects a weakening of trade winds associated with the developing El Niño event. Similar anomalous anticyclone is found in the middle troposphere (Fig. 2e), except the subtropical anticyclone ridgeline in 1991 shifts more northward and westward than the climatological mean. Although an anomalous anticyclone is also observed in the upper troposphere, its location significantly shifts northward compared to the lower and middle troposphere (Fig. 2f). Likewise, the upper tropospheric easterly anomalies related to the El Niño event occur over the equatorial western Pacific. The aforementioned anomalous anticyclone and an anomalous cyclone to its northeast appear to form an equivalent-barotropic wave-like pattern. Such a wave train pattern can be seen clearly in the Northern Hemisphere 500-hPa geopotential height anomalies (Fig. 3). Downstream are the subsequent positive and negative centers over Aleutian Islands and east of Hawaii, respectively. Huang and Sun (1992) found that the atmospheric circulation anomalies over East Asia and the Yangtze rainfall anomalies are simultaneously correlated with the convective activity around the Philippine Sea. Based on the general circulation model simulation, they suggested that this convective activity is largely driven by the SST anomaly in the western Pacific warm pool, which triggers a teleconnection

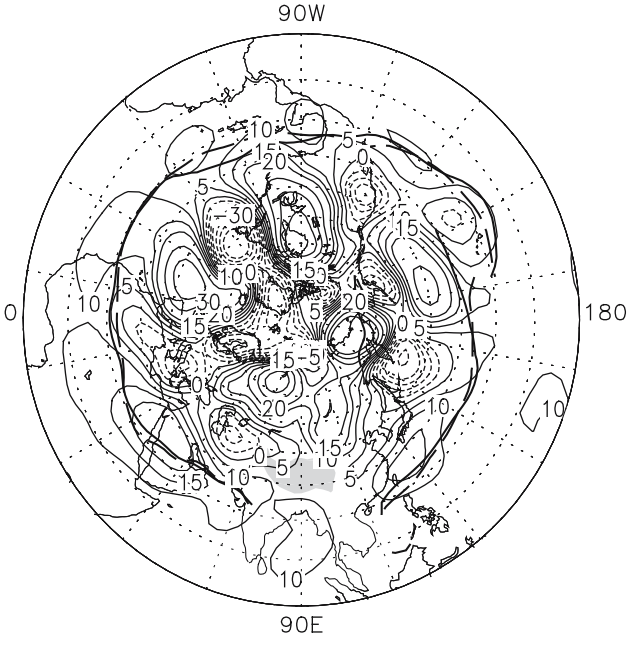

Fig. 3 500-hPa geopotential height anomalies (m) in the Northern Hemisphere for the 1991 summer. Anomalies are calculated as departures from the 1968 to 1996 base period seasonal means. *Thick solid* (*dashed*) *line* denotes the subtropical anticyclone ridgeline for the summer of 1991 (climatology). *Shading* indicates the Tibetan Plateau above 3,000 m

pattern, and, thus, leads to a drought or flood over the Yangtze Basin. It is intuitively obvious that the wave-like pattern during the 1991 summer might be closely related to the El Niño event.

3.3 Intraseasonal variations in rainfall

To show the anomalous intraseasonal variability during the summer of 1991, Fig. 4 illustrates time–latitude cross sections of the daily rainfall averaged over eastern China in climatology and in 1991. Climatologically, the Meiyu period around 30°N occurs between mid-June and mid-July (Tao and Chen 1987). Here it can be identified based on the criterion that the precipitation rate exceeds 6 mm day^{-1}. Within this Meiyu period, though the rainfall intensity appears different, no any significant period is identified based on the wavelet analysis, namely significant intraseasonal signal does not exist in the climatological Meiyu rainfall. But over the south of 25°N, the climatological intraseasonal fluctuations are more evident based on daily data in this study than those based on 10-day mean data reported by Lau et al. (1988). Compared to the climatological seasonal march of rainfall over eastern China, strong ISOs of the Yangtze rainfall are present during the 1991 summer. A distinct alternation of active and break sequences of rainfall is observed along 30–34°N. In southern China, the intraseasonal variations are also pronounced, and they seem to be out of phase with those over the Yangtze Basin. Such a north–south fluctuation of rainfall between these two latitudinal locations is similar to those in 1979 and in 1989 illustrated by Chen et al. (2000).

Based on Figs. 1 and 4, the area-averaged rainfall over the middle and lower Yangtze Basin (30–34°N, 115–120°E) is defined as a rainfall index to represent the extratropical East Asian summer monsoon. The area of this rainfall index is chosen for the region where both maximum percentage rainfall and maximum subseasonal standard deviation appear. The time series of the rainfall index is displayed in Fig. 5a. The evolution and intensity of this rainfall index exhibit distinct ISOs.

4 Intraseasonal variations in rainfall and circulation fields

4.1 Identifying intraseasonal oscillations

A wavelet analysis is applied to the time series of the Yangtze rainfall index to identify the dominant

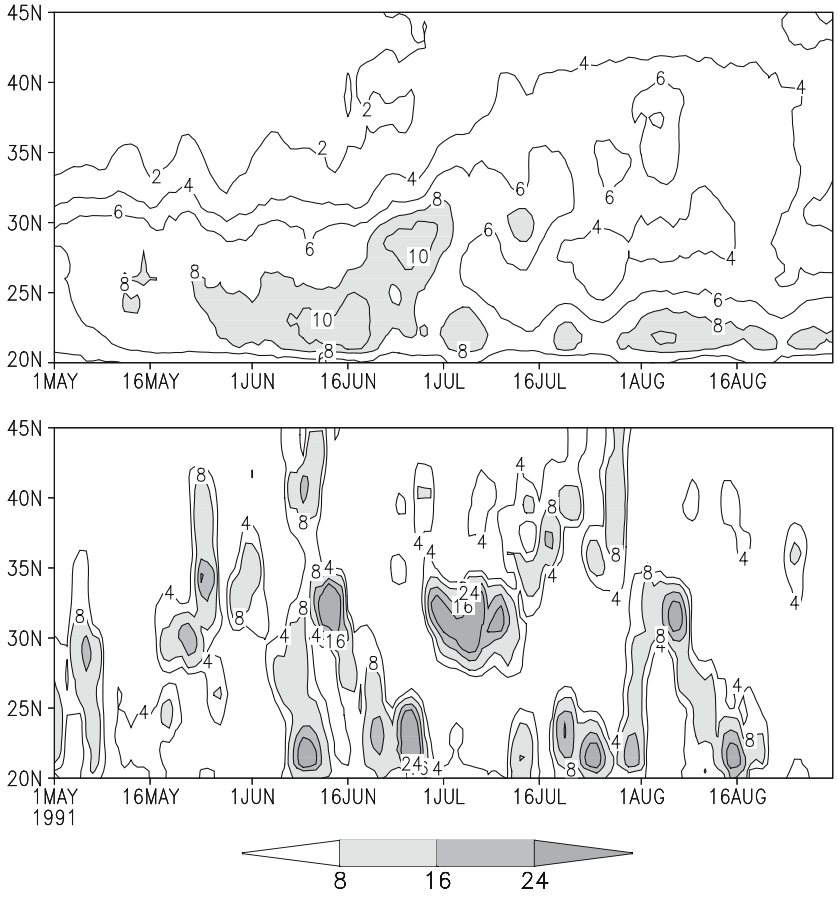

Fig. 4 Time-latitude cross section (115–120°E) of daily rainfall (mm day^{-1}) for the summer of climatology (*upper panel*) and 1991 (*lower panel*) from 1 May to 31 August. The climatology is based on the period 1951–1998. The rainfall values greater than 8 mm day^{-1} are *shaded*

intraseasonal periods. Figure 5b shows the wavelet spectrum. Significant spectral coefficients are concentrated within a band of 15–35 days, with significant variance in the 15–35-day band above 95% confidence level for red noise. The time series of the 15–35-day oscillation with four significant cycles illustrated in Fig. 5a is reconstructed by the inverse transform over all scales between 15 and 35 days. The close correlation between the time series of unfiltered rainfall and its 15–35-day filtered component indicates that this ISO accounts for almost half (actually 47%) of the total variance, suggesting that the 15–35-day oscillation is a dominant mode in the Yangtze Basin rainfall during the 1991 summer. Such a 15–35-day ISO is very different from those in other years. For example, Chen et al. (2000) reported that in 1989, the 12–24-day oscillation is pronounced in the Yangtze Basin rainfall, while in 1979, the 30–60-day oscillation is dominant. The 30–60-day mode is also found to influence the 1998 floods over eastern China (Zhu et al. 2003). We have also examined other summers, but the results do not show any significant signals in 15–35-day period. It should be mentioned that during the 1991 summer especially in active phases, the synoptic scale disturbances have also important contribution to rainfall variability. Indeed, the synoptic component less than 10 days explains 41% of the total variance.

Following Chan et al. (2002), an ISO cycle is defined as one with a positive and a negative anomaly (or an active and a break period), both of which must have a

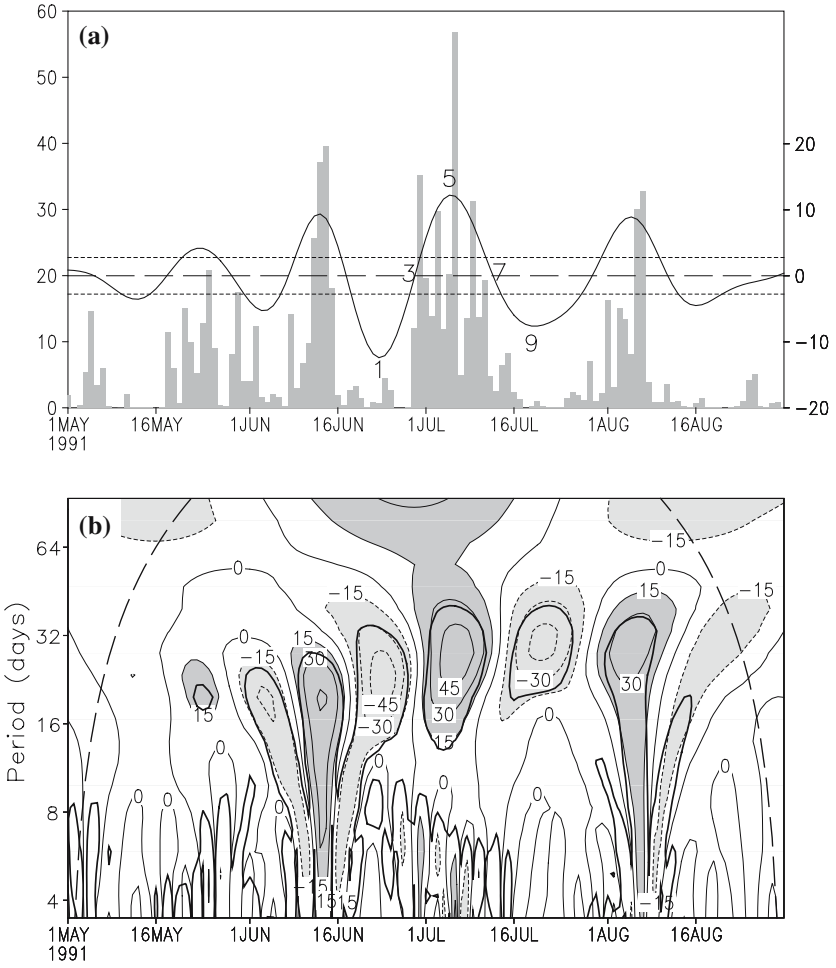

Fig. 5 **a** Histogram is the time series of the area-averaged (30–34°N, 115–120°E) daily rainfall (mm day^{-1}, with scale on the left-hand ordinate) used for the wavelet analysis. *Solid line* is the time series of the 15–35-day filtered daily rainfall anomalies (mm day^{-1}, with scale on the right-hand ordinate). The *thin dashed parallel lines* denote half of one standard deviation of the 15–35-day oscillation. Numbers *1, 3, 5, 7* and *9* represent the phases of the 15–35-day oscillation (see Sect. 4a for details). **b** Wavelet spectrum of the daily rainfall time series (*histogram*) in **a** using the six-order derivative of a Gaussian as wavelet basis function. The absolute values of the spectrum coefficients greater than 15 are *shaded*. *Thick solid* contour encloses regions of greater than 95% confidence for a red-noise process with a lag–1 coefficient of 0.90. *Thick dashed line* indicates the cone of influence outside which the edge effects become important (Torrence and Compo 1998)

peak amplitude greater than half of one standard deviation from zero. Based on this criterion, four significant cycles are selected. Then each cycle is divided into nine different phases (see Fig. 5a) for compositing as in Mao and Chan (2005). Phase 1 presents the peak of the break period while phase 3 represents the transition from a break to an active period. Phase 5 indicates the peak of active period and phase 7 is the transition from the active to the break period. Phases 2, 4, 6 and 8 occur at the time when the oscillation reaches half of its maximum or minimum value. Phase 9 is the same as Phase 1. The differences in the atmospheric circulation pattern for the extreme monsoon conditions can then be examined based on case study and composite analysis.

4.2 Circulation characteristics during the active and break phases

The evolution of the 15–35-day filtered rainfall displayed in Fig. 5a clearly shows that the cycle during 23 June–19 July possesses the largest amplitude among the four cycles. Therefore, this cycle is chosen to investigate the atmospheric circulation features for the break and active periods. To avoid redundancy, the flow patterns are illustrated only for the two extreme monsoon conditions when the filtered Yangtze rainfall index reaches its minimum (maximum). Figure 6 shows the strongest case, and Fig. 7 shows the composite results. In order to remove high-frequency fluctuations, the wind components are averaged for the 3 days centered on each phase. During the extreme break phase (phase 1, centered on 23 June), the unfiltered 850-hPa winds show that the subtropical anticyclone, with the westernmost point of its ridgeline locating around 130°E, appears over the western North Pacific (Fig. 6a). Strong monsoon westerlies prevail over the SCS due to northward extension of the subtropical anticyclone, while northeasterlies dominate over most of southern China in such a way that the middle and lower Yangtze Basin is controlled by divergent circulation. In the upper troposphere (Fig. 6e), the South Asian anticyclone situates over the Tibetan Plateau, and another anticyclone exists over the western North Pacific. A meridional deep trough occurring between these two anticyclones stretches southward into southern China, forming a convergence environment over the Yangtze Basin. It dynamically corresponds to the 850-hPa divergent wind field, which is inconducive to the occurrence of heavy rainfall. The 15–35-day filtered 850-hPa winds show that there is an anomalous cyclone centered near Taiwan (Fig. 6b). In the filtered 200-hPa winds, there exists a dipole anomaly characterized by anomalous cyclone over eastern China and anomalous anticyclone over the northern Tibetan Plateau. Also observed is another broad anticyclone covering most of the western North Pacific (Fig. 6f).

In contrast, during the extreme active phase (phase 5, centered on 6 July), the subtropical anticyclone intrudes southwestward into the northern SCS, with its westernmost point of the ridgeline reaching west of 110°E. The monsoon southwesterlies prevail over southern China, leading to an increased moisture convergence along the Yangtze Basin (Fig. 6c). The South Asian anticyclone at the 200-hPa extends to east of 130°E. It is largely zonally-oriented, and its ridgeline is located near 25°N (Fig. 6g). There exists a local vertical meridional monsoon cell over eastern China characterized by northeasterlies in the upper troposphere and southwesterlies in the lower troposphere, which favors an active Meiyu. An anomalous anticyclone centered around the Bashi Channel (20°N, 121°E) is observed over the northern SCS through the Philippine Sea in the filtered 850-hPa wind field (Fig. 6d). The filtered 200-hPa winds show that the dipole anomaly becomes a dominant system, while the anticyclone over the western North Pacific weakens significantly (Fig. 6h). The anticyclone over China is just located northwest of the anomalous 850-hPa anticyclone in such a way that the northeasterly anomalies in the upper-levels overlap the southwesterly anomalies in the low-levels along eastern coasts of China.

The variations of the atmospheric circulation can be further corroborated based on composite winds. The composites are calculated by averaging the wind components on the corresponding dates of the four significant cycles. Similar to the case patterns, during the extreme break phase, the subtropical anticyclone retreats eastward so that the monsoon westerlies mainly run toward the SCS (Fig. 7a), in the upper troposphere the South Asian anticyclone shrinks westward with its ridgeline along 20°N (Fig. 7e). During the active phase, the tropical monsoon westerlies veer to northeast over the northern SCS due to the southwestward intrusion of the subtropical anticyclone ridge so that the SCS monsoon trough is filled. Thus the enhanced monsoon southwesterlies converge toward the Yangtze Basin (Fig. 7c). In the upper levels a strong, northeastward-extended easterly jet helps to initiate intense convective activity along the Meiyu front (Fig. 7g). The composite patterns of the filtered winds resemble those occurring in the extreme cases. In the break phase, a significantly anomalous cyclone centered over the western Philippine Sea exists in the lower troposphere (Fig. 7b), and a dipole anomaly

is present in the upper troposphere (Fig. 7f). The opposite variations are found in the active phase (Fig. 7d, h).

The importance of the intraseasonal mode in terms of dynamic conditions can be further illustrated from the evolutions of the filtered 850-hPa relative vorticity and the 200-hPa divergence (Fig. 8). Because the filtered lower-level relative vorticity is significantly negatively-correlated with the filtered upper-level divergence with correlation coefficient of –0.77, these two dynamic factors exhibit an in-phase variation, reflecting the evolutions of the above-stated coupled anomalous flow pattern. Based on the atmospheric continuity equation, a strong divergence in the upper troposphere produces an enhanced ascending motion in the middle troposphere, leading to increased rainfall. These suggest that the variations of the Yangtze rainfall rely heavily on the coupling between the lower-level relative vorticity and the upper-level divergence. Note that the filtered Yangtze rainfall is also highly correlated with the lower-level relative vorticity, with a correlation coefficient exceeding 0.95. This indicates that the low-level forcing plays an important role in regulating the Yangtze rainfall during the 1991 summer.

The above results suggest that the break (active) phase of the 15–35-day oscillation manifests as an anomalous cyclone (anticyclone) in the lower troposphere existing alternatively over the northern SCS through the Philippine Sea, which modulates the northeastward (southwestward) shift of the WPSH in the SCS, forming a lower tropospheric divergence (convergence) over the Yangtze Basin. The upper tropospheric dipole anomaly is characterized by an anomalous cyclone (anticyclone) over eastern China and an anomalous anticyclone (cyclone) over the northern Tibetan Plateau, which regulates the southwestward shrinking (northeastward extending) of the South Asian anticyclone, causing an upper tropospheric convergence (divergence) over eastern China. According to the atmospheric continuity equation, such a coupled flow pattern between the lower and the upper troposphere favors large-scale descending (ascending) motion in the troposphere, thus leading to the reduction (enhancement) in rainfall over the Yangtze Basin. Therefore, the 15–35-day ISO is the major agent in regulating the Yangtze rainfall during the 1991 summer. Recall that in summer the South Asian high at 100 hPa and the WPSH at 500 hPa tend to move in a contrary direction (Tao and Zhu 1964). The present results demonstrate that such a movement also exists between the upper and lower tropospheric subtropical highs on intraseasonal time scales.

Fig. 6 **a** Unfiltered and **b** filtered 850-hPa winds (m s^{-1}) for extreme break phase (indicated by number 1 in Fig. 5a); **c**, **d** as in **a**, **b** but for extreme active phase (indicated by number *5* in Fig. 5a); **e**–**h** as in **a**–**d** except for 200-hPa winds. *Thick solid line* denotes the subtropical anticyclone ridgeline. *Thick dashed line* is the 3,000-m orographic contour of the Tibetan Plateau ▶

4.3 Association with ISO of the 500-hPa geopotential height

Previous studies have emphasized the impacts of the subtropical high at 500 hPa on the surrounding weather and climate (e.g. Huang and Yue 1962; Huang and Sun 1992; Chang et al. 2000a, b). Figure 9 shows the distributions of the lagged correlation with lags of every 3 days between the filtered Yangtze rainfall index and the 500-hPa geopotential height field since the time span of 25 days (from day –12 to day +12) is roughly a complete cycle of the 15–35-day mode. To reveal the regions where the intraseasonal scale anomalies occur around and within the subtropical high, the summer mean 500-hPa geopotential height field is plotted as circulation background.

A significantly negative correlation area is observed over the northern SCS-East China Sea on Day –12, and almost disappears after 3 days. This negative correlation occurs over the western part of the summer mean North Pacific subtropical high, suggesting that the intraseasonal variations in the WPSH in the middle troposphere is closely related to the Yangtze rainfall. This negative correlation area also corresponds to the aforementioned 850-hPa anomalous cyclone (anticyclone) during the break (active) phase. More interestingly, a significantly positive correlation area is found over north of Hawaii, where the ridgeline of the summer mean North Pacific high is discontinuous. This indicates an intraseasonal teleconnection between the Yangtze rainfall anomalies and the circulation anomalies in the North Pacific subtropical high over north of Hawaii. Subsequently, the positive correlation area extends significantly westward, forming a larger positive correlation region in a southwest–northeast oriented band that covers most of central-western North Pacific from 140°W to 130°E on Day –9. The positive correlation continues to propagate westward into the SCS by Day –6, and eventually vanishes over southern China at Day +6. When the major positive correlation propagates westward, a small region with moderately negative values appears on Day –4 around Hawaii. This newly developed negative correlation region grows as it repeats the chronicle and itinerary of the aforementioned positive correlation region. It is also found that from one extreme phase to another, the

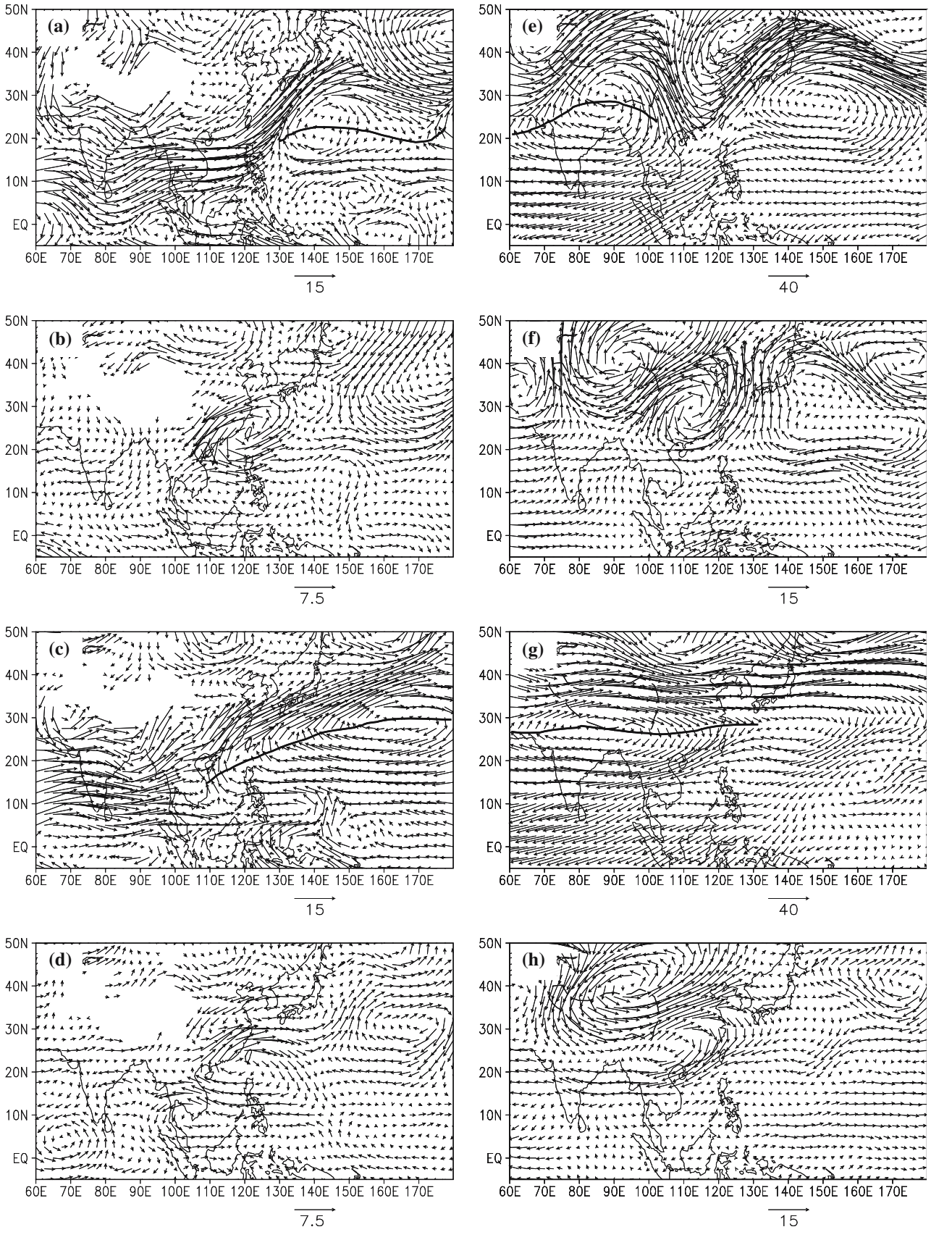
(a)
(b)
(c)
(d)
(e)
(f)
(g)
(h)
50N
40N
30N
20N
10N
EQ
60E 70E 80E 90E 100E 110E 120E 130E 140E 150E 160E 170E
15
7.5
15
7.5
40
15

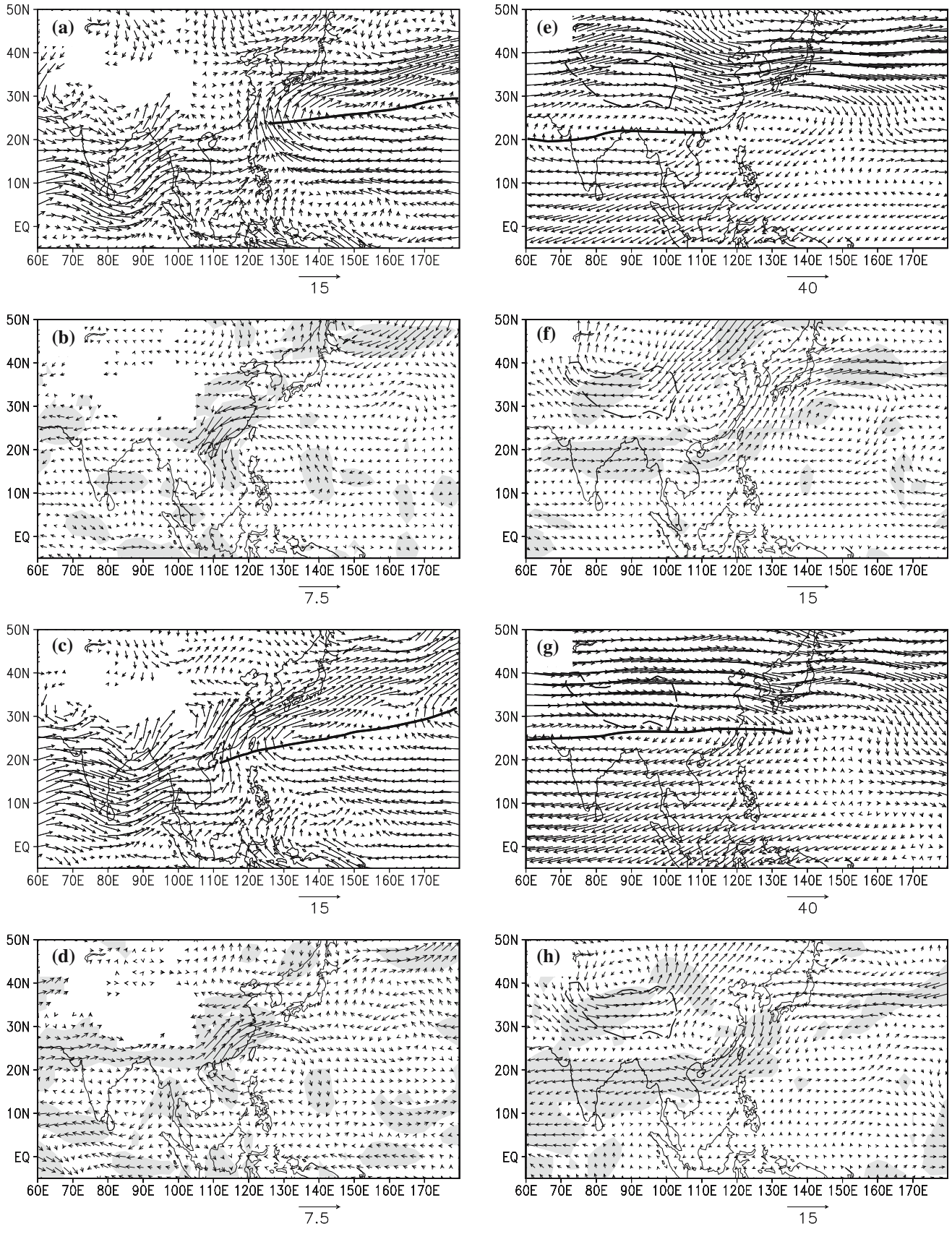
(a)
(b)
(c)
(d)
(e)
(f)
(g)
(h)
50N
40N
30N
20N
10N
EQ
60E 70E 80E 90E 100E 110E 120E 130E 140E 150E 160E 170E
15
7.5
40

◀ **Fig. 7** Same as Fig. 6, but for composite wind fields. The composites are calculated by averaging the wind components on the corresponding dates of the four ISO cycles. *Shading* indicates grid points where the filtered wind anomalies are significantly different from zero at the 95% level (based on the *t* test) in at least one of the wind components (zonal or meridional)

anomalies originating from the central North Pacific north of Hawaii propagates westward along the easterly background flow on the south of the WPSH. The evolutions of the correlation patterns show that the Yangtze rainfall is linked with the ISO events in the North Pacific subtropical high. The 15–35-day oscillation in the subtropical high tends to propagate westward along the easterly background flow from north of Hawaii to the northern SCS, dictating the break and active sequences of the Yangtze rainfall.

To demonstrate more clearly the westward propagation of the 15–35-day oscillation, the time–latitude cross sections of the 15–35-day filtered geopotential height at 500-hPa are illustrated in Fig. 10. Of interest to us is the height anomalies around the northern SCS and their origin, then the three longitude bands are selected from east to west based on Fig. 9. From Fig. 10c, four positive centers along with negative centers are found between 10 and 25°N, which are well corresponding to the peak phases shown in Fig. 5a. The corresponding anomaly centers exist over other longitudes (Fig. 10a, b). Tracing the corresponding positive centers at different longitudes for every ISO cycle, the westward propagation of the ISO is evident. During an ISO cycle, a positive (negative) anomaly center over the central North Pacific is concurrent with a negative (positive) one over the western North Pacific, indicating that the former leads the latter by half period.

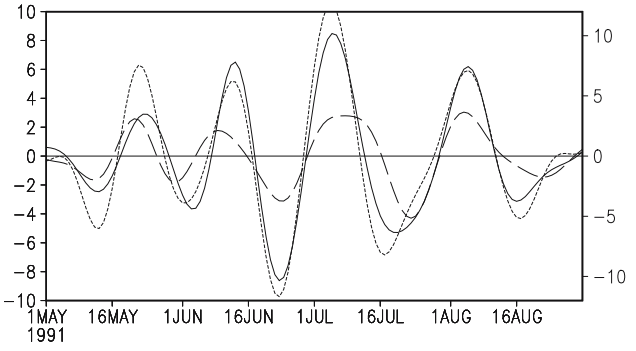

Fig. 8 Time series of the 15–35-day filtered daily rainfall (mm day^{-1}, *solid line*), 850-hPa relative vorticity (10^{-6} s^{-1}, *short dashed line*) and 200-hPa divergence (10^{-6} s^{-1}, *long dashed line*) anomalies over the Yangtze Basin (30–34°N, 115–120°E). The scale on the right-hand ordinate is for rainfall, while that on the left-hand ordinate for vorticity and divergence

These suggest that the positive (negative) height anomalies over the northern SCS-Philippine Sea, which favor an active (break) Yangtze rainfall (Fig. 9), are originated from the central North Pacific north of Hawaii. It seems that there are some signals from the equator or higher latitudes such as in the third and the fourth ISO cycles, and these signals have some contributions to the western North Pacific height anomalies. But the dominant signal is from the central North Pacific. As to how the geopotential height anomalies are generated over central North Pacific, this question needs to be studied for the future.

5 Summary and discussion

During the 1991 summer, devastating floods caused by a series of heavy rain events occur over the middle and lower Yangtze Basin, with the total summer rainfall being at least 50% more than normal. The Yangtze rainfall exhibits considerable intraseasonal variability with several active and break sequences in intensity. Therefore, the area-averaged rainfall over the middle and lower Yangtze Basin is selected as a reference parameter to identify the ISOs in the extratropical East Asian summer monsoon. The objective of this paper is to examine the atmospheric circulation features in relation to the intraseasonal variability of the Yangtze rainfall for a better understanding of the causes of the extreme flood.

Wavelet analysis shows that the 15–35-day oscillation is the dominant mode that controls the Yangtze rainfall during the 1991 summer. Based on the amplitude of the 15–35-day oscillation of the Yangtze rainfall, four significant cycles are identified with the largest amplitude appearing from 23 June to 19 July. An examination of circulation features suggests that the 15–35-day oscillation exhibits an anomalous cyclone (anticyclone) in the lower troposphere existing alternatively over the northern SCS through the Philippine Sea. It modulates a southwest–northeast migration of the western Pacific subtropical anticyclone over the SCS, leading to a low-level divergence (convergence) over the Yangtze Basin. The upper tropospheric dipole anomaly is characterized by an anomalous cyclone (anticyclone) over eastern China and an anomalous anticyclone (cyclone) over the northern Tibetan Plateau, which regulates a southwestward shrinking (northeastward extending) of the South Asian anticyclone, resulting in an upper-level convergence (divergence) over eastern China. Based on the atmospheric continuity equation, such a coupled flow pattern between the lower and the upper

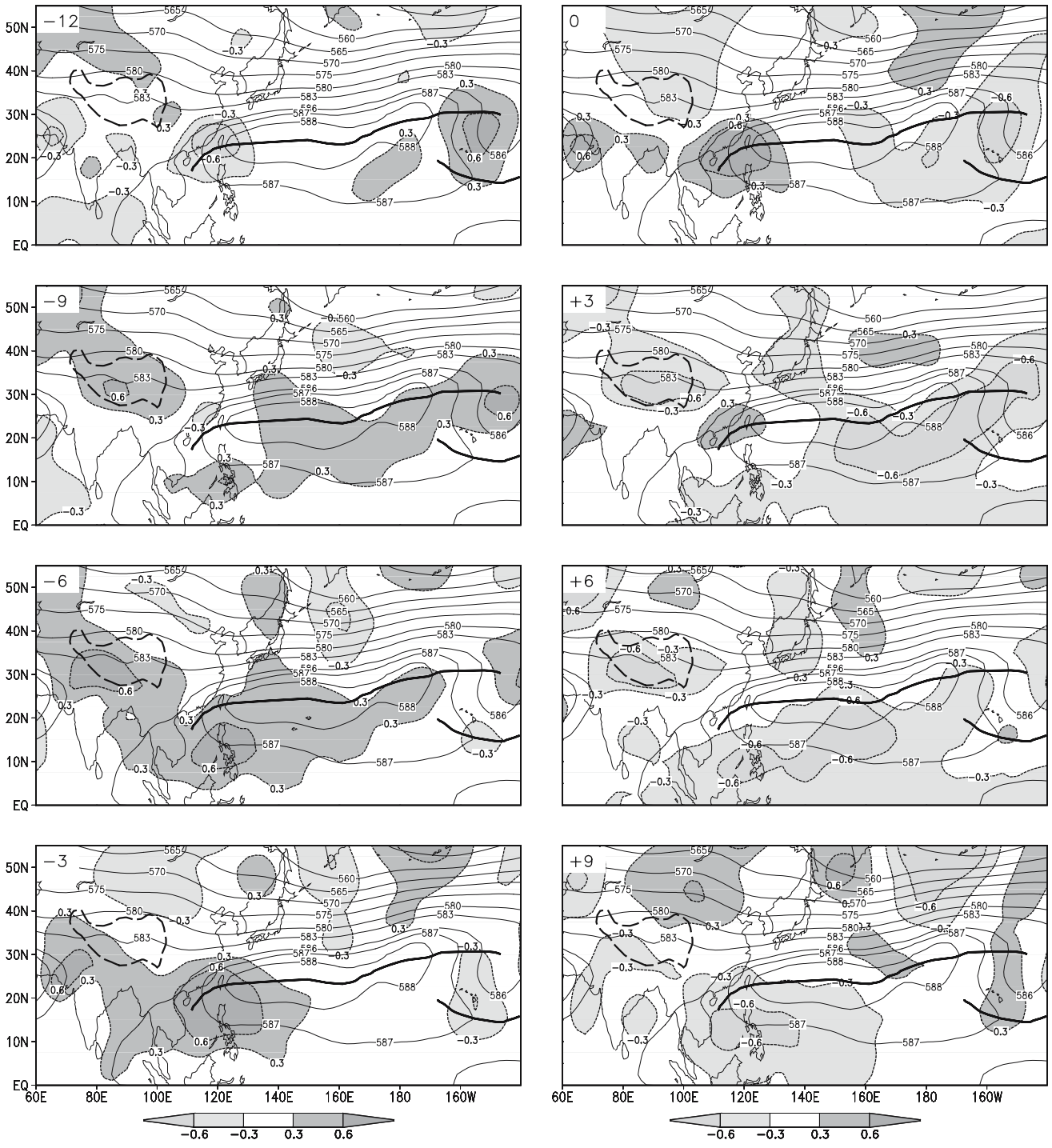

Fig. 9 Lagged correlations (*thin dashed* contour and *shading*) between the 15–35-day filtered Yangtze rainfall index and the 15–35-day filtered 500-hPa geopotential height superimposed on the summer (1 May–31 August 1991) mean 500-hPa geopotential height field (dam, *thin solid contour*). Critical positive (negative) values of the correlation exceeding the 95% significance level are *darkly* (*lightly*) *shaded*. *Thick solid line* indicates the subtropical anticyclone ridgeline. *Thick dashed line* is the 3,000-m orographic contour of the Tibetan Plateau. Negative lag such as *-12* indicates that the geopotential height leads the rainfall, the opposite for positive lag

troposphere favors large-scale descending (ascending) motion in the troposphere, leading to the reduction (enhancement) in rainfall along the Yangtze Basin. Dynamically, the intraseasonal variations in the Yangtze rainfall are mainly determined by the coupling between the low-level relative vorticity and the

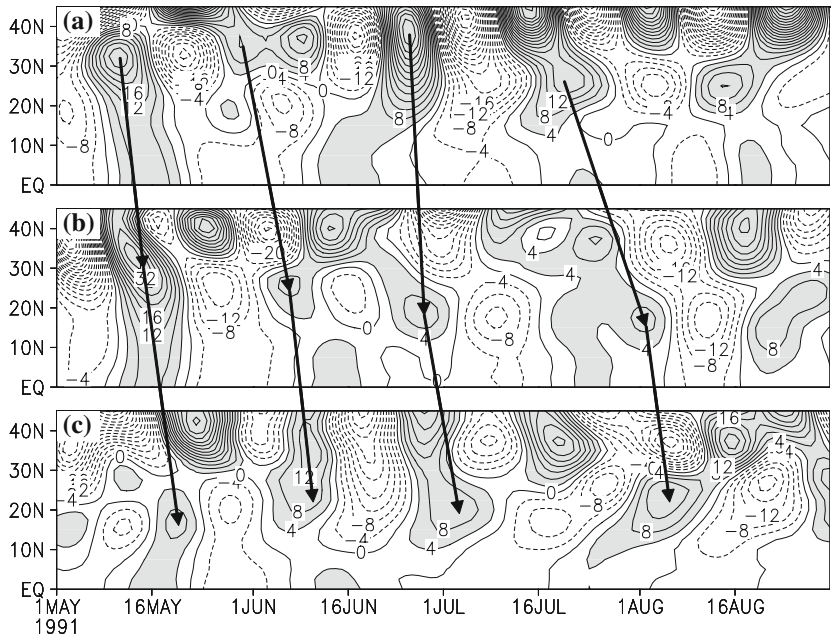

Fig. 10 Time-latitude cross sections of the 15–35-day filtered 500-hPa geopotential height anomalies (m) for the different longitudes. **a** 155–160°W, **b** 150–155°E, and **c** 125–130°E. Positive anomalies greater than 4 m are *shaded*. *Arrows* indicate the propagation direction of the ISOs

upper-level divergence. The 15–35-day oscillation of the Yangtze rainfall is in phase with the lower tropospheric relative vorticity. It is demonstrated that in summer an opposite movement exists between the South Asian high in the upper troposphere and the WPSH in the lower troposphere on intraseasonal time scales.

The correlation and case studies show that the active and break periods of the Yangtze rainfall are closely associated with the 15–35-day ISOs in the North Pacific subtropical high at 500 hPa. The 15–35-day oscillations in the subtropical high originates from the central North Pacific north of Hawaii, and tend to propagate westward along the easterly background flow toward the northern SCS through the Philippine Sea, affecting the break and active sequences of the Yangtze rainfall. Considering the activities of the 15–35-day oscillations in the atmosphere circulation associated with the extratropical East Asian monsoon, it may be suggested that the Yangtze floods in 1991 are to a great extent related to such strong ISOs.

It should be mentioned that this research is only a case study, and the situation may not be similar to all other years. But the present results could provide basic scenario for further investigation into other possible physical processes, such as how and to what extent the El Niño event and the middle–high latitude circulation systems can modulate the Yangtze rainfall on intraseasonal time scales. Of course, the mechanisms responsible for the intraseasonal variability of the North Pacific subtropical high and its teleconnection with the El Niño event also deserve further study based on more cases. Besides, some possible mechanisms need to be verified using numerical modeling.

Acknowledgments The NCEP/NCAR reanalysis data are provided by the NOAA-CIRES Climate Diagnostics Center, Boulder, Colorado, USA, from their Web site at http://www.cdc.noaa.gov/. This research was supported by the National Basic Research program of China (Grant No.2005CB422004) and Natural Science Foundation of China under Grants 40375022, 40135020, 40325015, and 40475027.

References

Chan JCL, Ai W, Xu J (2002) Mechanisms responsible for the maintenance of the 1998 South China Sea summer monsoon. J Meteor Soc Jpn 80:1103–1113

Chang CP, Zhang Y, Li T (2000a) Interannual and interdecadal variations of the East Asian summer monsoon and tropical Pacific SSTs. Part I: Roles of the subtropical ridge. J Clim 13:4310–4325

Chang CP, Zhang Y, Li T (2000b) Interannual and interdecadal variations of the East Asian summer monsoon and tropical Pacific SSTs. Part II: Meridional structure of the monsoon. J Clim 13:4326–4340

Chen TC, Yen MC, Weng SP (2000) Interaction between the summer monsoon in East Asia and the South China Sea: intraseasonal monsoon modes. J Atmos Sci 57:1373–1392

Fukutomi Y, Yasunari T (1999) 10–25-day intraseasonal variations of convection and circulation over East Asia and western North Pacific during early summer. J Meteor Soc Jpn 77:753–769

Fukutomi Y, Yasunari T (2002) Tropical–extratropical interaction associated with the 20–25-day oscillation over the western Pacific during the northern summer. J Meteor Soc Jpn 80:311–331

Hoskins BJ (1996) On the existence and strength of the summer subtropical anticyclones. Bull Am Meteor Soc 77:1287–1292

Hsu HH (2005) East Asian monsoon. In: Lau KM, Waliser DE (eds) Intraseasonal variability in the atmosphere–ocean climate system, Springer, Berlin Heidelberg New York, pp 63–94

Huang R, Wu Y (1989) The influence of ENSO on the summer climate change in China and its mechanism. Adv Atmos Sci 6:21–32

Huang R, Sun F (1992) Impacts of the tropical western Pacific on the East Asian summer monsoon. J Meteor Soc Jpn 70:342–256

Huang S, Yue T (1962) On the structure of the subtropical highs and some associated aspects of the general circulation of atmosphere (in Chinese). Acta Meteorol Sinica 31:339–359

Kalnay E, Coauthors (1996) The NCEP/NCAR 40-year reanalysis project. Bull Am Meteor Soc 77:437–471

Lau KM, Weng H (1995) Climate signal detection using wavelet transform: how to make a time series sing. Bull Am Meteor Soc 76:2391–2402

Lau KM, Yang GJ, Shen SH (1988) Seasonal and intraseasonal climatology of summer monsoon rainfall over East Asia. Mon Weather Rev 116:18–37

Lau KM, Yang S (1996) Seasonal variation, abrupt transition, and intraseasonal variability associated with the Asian summer monsoon in the GLA GCM. J Clim 9:965–985

Liu Y, Wu G, Liu H, Liu P (2001) Condensation heating of the Asian summer monsoon and the subtropical anticyclone in the Eastern Hemisphere. Clim Dyn 17:327–338

Lu E, Ding Y (1997) Analysis of summer monsoon activity during the 1991 excessively torrential rain over Changjiang-Huahe river valley (in Chinese). Quart J Appl Meteor 8:317–324

Mao J, Chan JCL (2005) Intraseasonal variability of the South China Sea summer monsoon. J Clim 18:2388–2402

McPhaden MJ (1993) TOGA-TAO and the 1991–93 El Niño Southern Oscillation event. Oceanography 6:36–44

Rodwell MR, Hoskins BJ (2001) Subtropical anticyclones and summer monsoons. J Clim 14:3192–3211

Tanaka M (1992) Intraseasonal oscillation and onset and retreat dates of the summer monsoon over East, Southeast Asia and the western Pacific region using GMS high cloud amount data. J Meteor Soc Jpn 70:613–629

Tao S, Chen L (1987) A review of recent research on the East Asian summer monsoon in China. In: Chang CP, Krishnamurti TN (eds) Monsoon meteorology, Oxford University Press, Oxford, pp 60–92

Tao S, Zhu F (1964) Variation of the 100 hPa flow pattern in South Asia in summer and the movement of the subtropical anticyclone over the western Pacific (in Chinese). Acta Meteorol Sinica 34:385–394

Tao S, Ding Y (1981) Observational evidence of the influence of the Qinghai-Xizang (Tibet) plateau on the occurrence of heavy rain and severe storms in China. Bull Am Meteor Soc 62:23–30

Torrence C, Compo GP (1998) A practical guide to wavelet analysis. Bull Am Meteor Soc 79:61–78

Webster PJ, Magana VO, Palmer TN, Shukla J, Tomas RA, Yanai M, Yasunari T (1998) Monsoons: processes, predictability, and the prospects for prediction. J Geophys Res 103(C7):14451–14510

Wu G, Liu Y, Liu P (1999) The effect of spatially non-uniform heating on the formation and variation of subtropical high. Part I: Scale analysis (in Chinese). Acta Meteorol Sinica 57:257–263

Wu G, Liu Y (2003) Summertime quadruplet heating pattern in the subtropics and the associated atmospheric circulation. Geophys Res Lett 30(5):1201. DOI:10.1029/2002GL016209

Yeh T, Tao S, Li M (1959) The abrupt changes of circulation over the Northern Hemisphere during June and October. In: Bolin B (eds) The atmosphere and the sea in motion. Rockefeller Institute Press and Oxford University Press, pp 249–267

Zhu C, Nakazawa T, Li J, Chen L (2003) The 30–60 day intraseasonal oscillation over the western North Pacific Ocean and its impacts on summer flooding in China during 1998. Geophys Res Lett 30(18):1952. DOI:10.1029/2003GL017817